National Technical University of Athens

Determination of the thermal conductivity of vacuum insulation panels at fire/elevated temperatures

D.A. Kontogeorgos[a,*], G.K. Semitelos[a], I.D. Mandilaras[a], R. Caps[b], L. Kubina[b] and M.A. Founti[a]

[a]*National Technical University of Athens, School of Mechanical Engineering, Lab. of Heterogeneous Mixtures and Combustion Systems*
[b]*Va-Q-Tec AG, Karl Ferdinand Braunstrasse 7, 97080 Wurzburg, Germany*

IVIS2015
12th International Vacuum Insulation Symposium - September 19 – 21, 2015, NUAA, Nanjing, P.R. China

- Introduction
- Experimental Methodology
- Numerical Modeling
- Results & Discussion
- Conclusions & Outlook

- Introduction
- Experimental Methodology
- Numerical Modeling
- Results & Discussion
- Conclusions & Outlook

- **Vacuum Insulation Panels**
  - Variety of applications such as refrigerator, transport, container, building applications etc.
  - Research has mainly focused on the thermal behavior under low temperatures
- **Building applications**
  - Growing interest in fire protection of buildings mainly due to the increase of legislation and fire standard restrictions
  - Assessment of building materials under fire temperatures is essential
  - Need for accurate physical properties for the “performance-based” fire codes
- **Growing Question: *What are the physical properties of VIPs at fire temperatures?***
- **Scope of this Work**: Define the thermal conductivity of VIP at fire temperatures
  - Integrated methodology were experimental values are coupled with detailed numerical model for the VIP’s thermal conductivity

- Introduction
- Experimental Methodology
- Numerical Modeling
- Results & Discussion
- Conclusions & Outlook

- Experimental methodology
  - Based on the heat flow meter apparatus method
- VIP samples
  - Two samples were joint together to form the final test specimen
- Sensors
  - Thermocouples: record temperature on the exposed and unexposed surfaces
  - Heat flux: record heat flux on the unexposed surface
- Specimen location
  - Positioned between two steel plates to ensure uniform temperature distribution on the surfaces

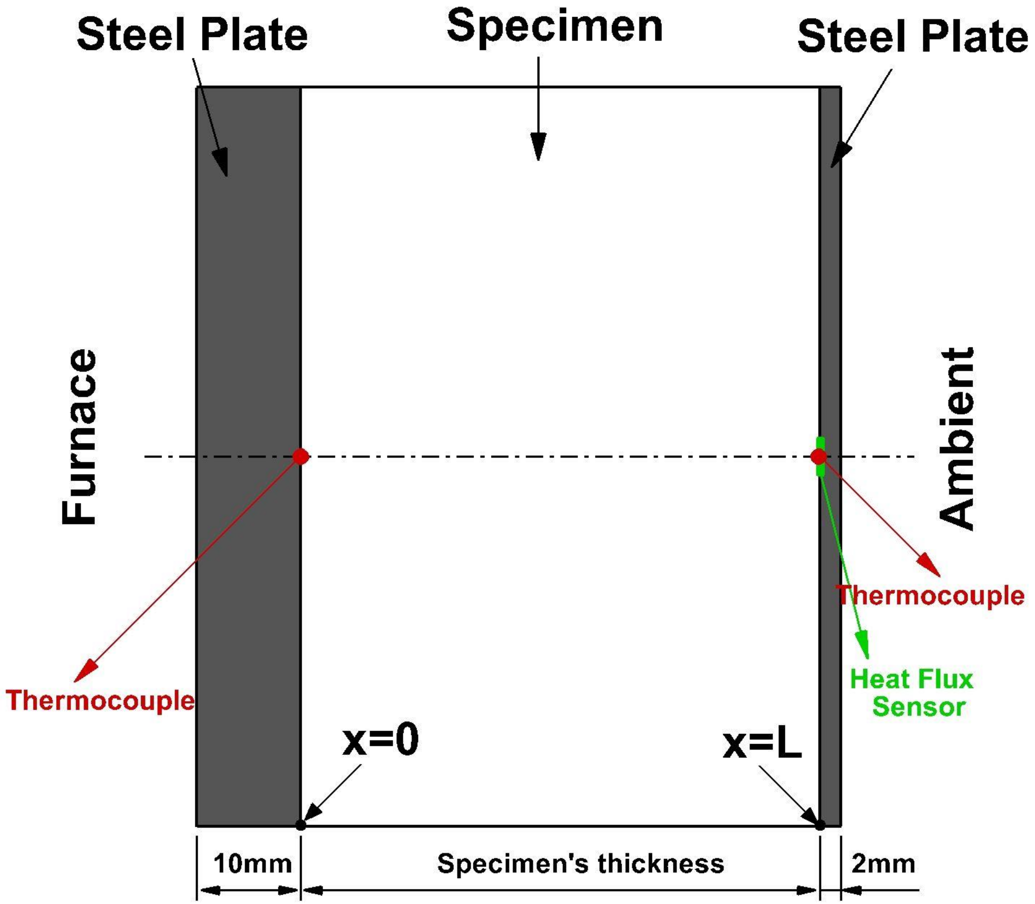

Schematic diagram of the experimental set up

- Experimental methodology
  - Based on the heat flow meter apparatus method
- VIP samples
  - Two samples were joint together to form the final test specimen
- Sensors
  - Thermocouples: record temperature on the exposed and unexposed surfaces
  - Heat flux: record heat flux on the unexposed surface
- Specimen location
  - Positioned between two steel plates to ensure uniform temperature distribution on the surfaces

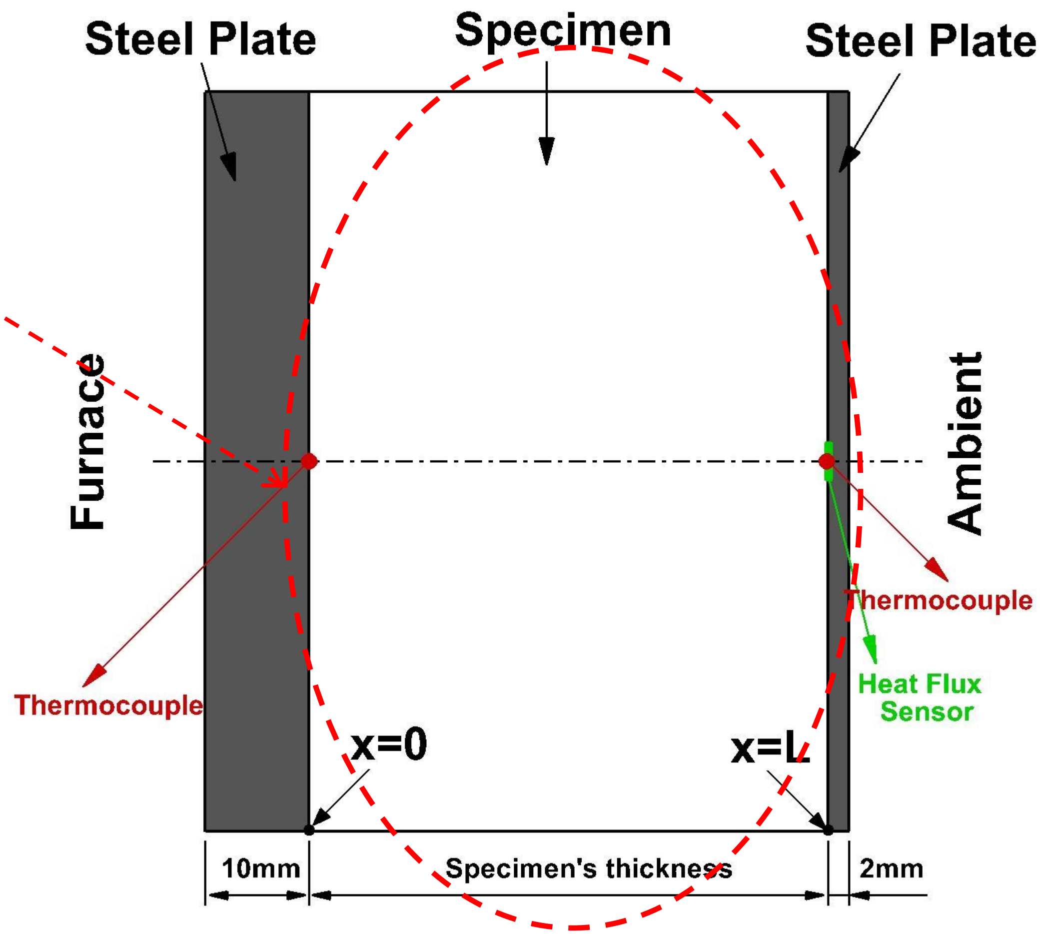

Schematic diagram of the experimental set up

- Experimental methodology
  - Based on the heat flow meter apparatus method
- VIP samples
  - Two samples were joint together to form the final test specimen
- Sensors
  - Thermocouples: record temperature on the exposed and unexposed surfaces
  - Heat flux: record heat flux on the unexposed surface
- Specimen location
  - Positioned between two steel plates to ensure uniform temperature distribution on the surfaces

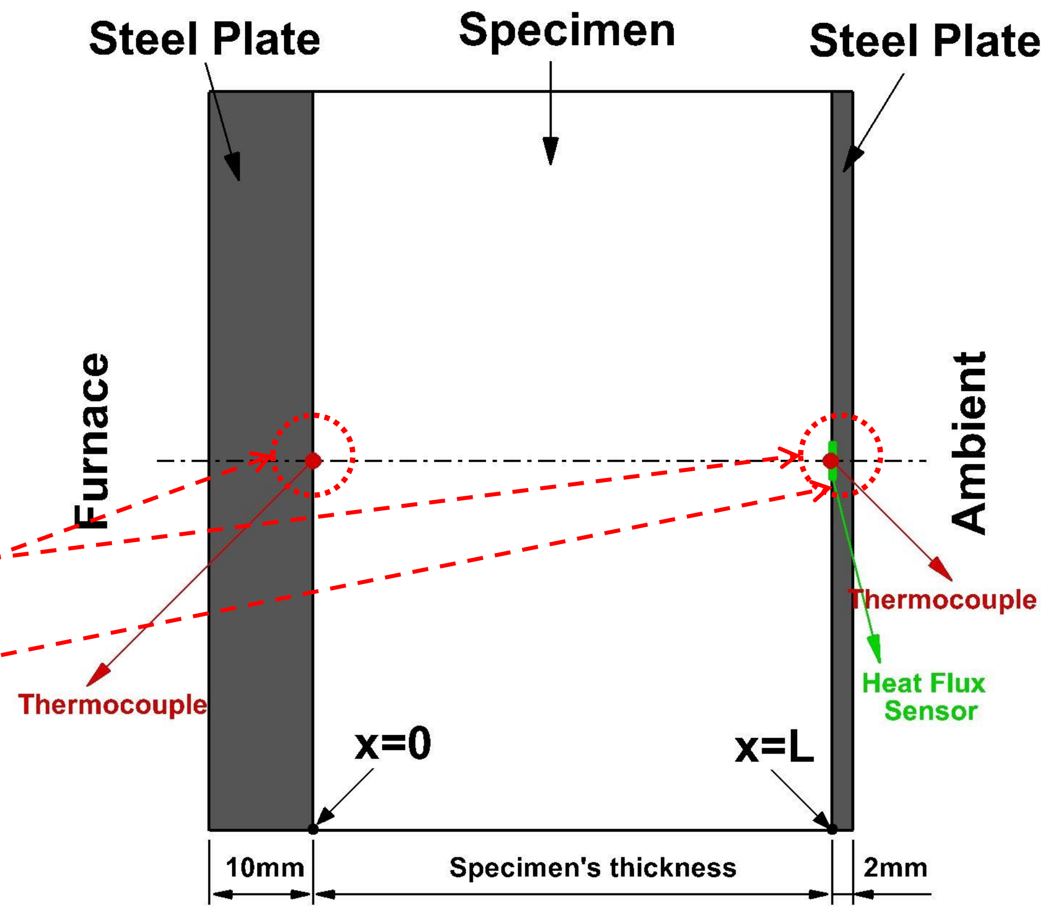

Schematic diagram of the experimental set up

- Experimental methodology
  - Based on the heat flow meter apparatus method
- VIP samples
  - Two samples were joint together to form the final test specimen
- Sensors
  - Thermocouples: record temperature on the exposed and unexposed surfaces
  - Heat flux: record heat flux on the unexposed surface
- Specimen location
  - Positioned between two steel plates to ensure uniform temperature distribution on the surfaces

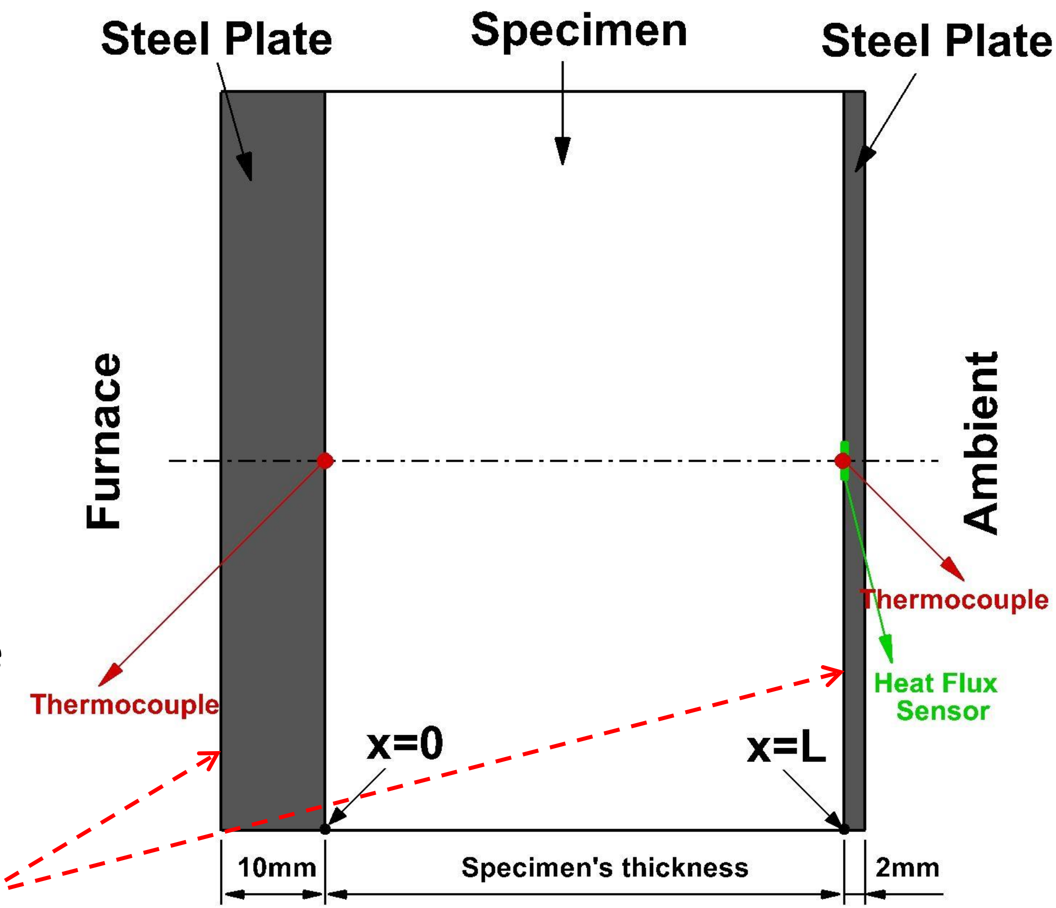

Schematic diagram of the experimental set up

- Total assembly
  - Placed inside a frame made from insulation material
    - Minimize lateral thermal losses
  - Positioned in front of a radiation furnace
    - One surface exposed to furnace’s thermal load and the other exposed to ambient conditions
- Agilent data acquisition unit (±2%)
  - Temperature and heat flux measurements

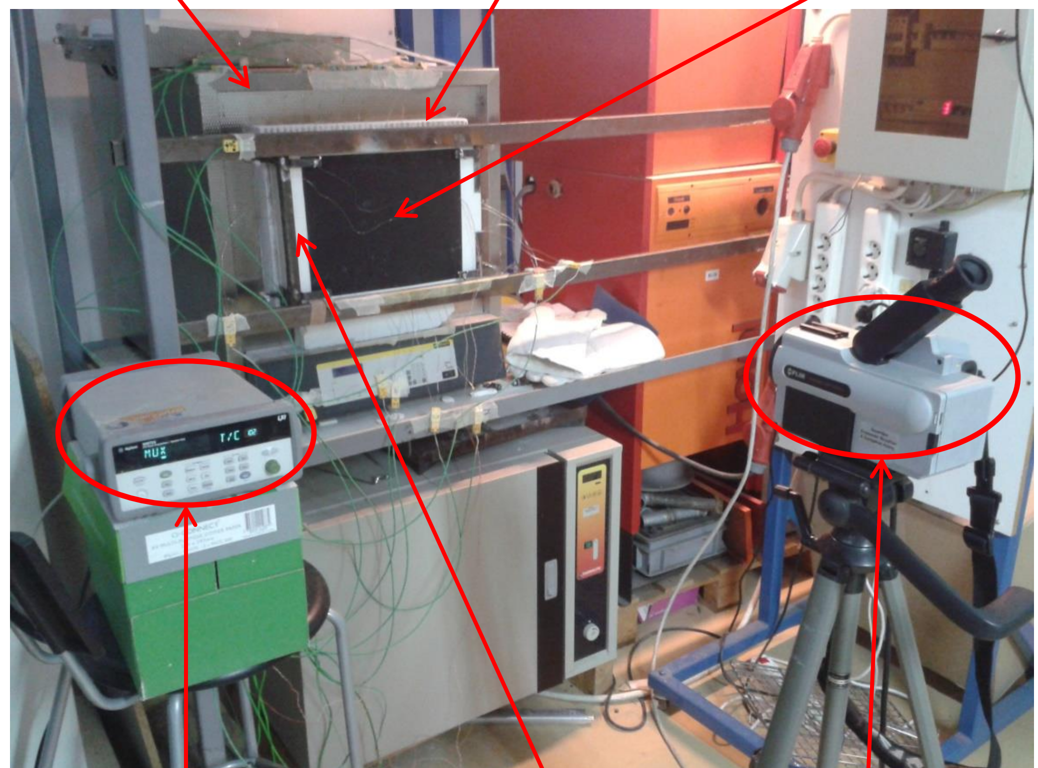

- Calibration of the experimental set up
  - Definition of calibration factor using reference material (i.e. Kaowool 1260 insulation)
  - Specify the influence of high temperatures
- Experimental Methodology
  - Furnace's temperature set to a desired level (range 100°C to 900°C with an interval of 100°C)
  - Temperature and heat flux evolution recorded until steady state conditions
  - Steady state values utilized for the determination of the thermal conductivity

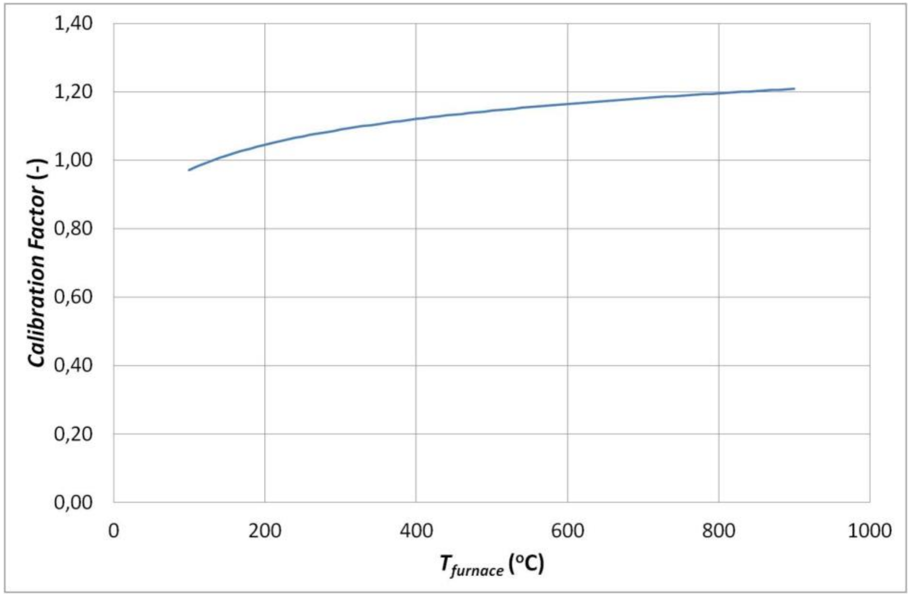

Calibration factor at different levels of the furnace's temperature

- Introduction
- Experimental Methodology
- **Numerical Modeling**
- Results & Discussion
- Conclusions & Outlook

Main Idea

- Approximations
  - One dimensional heat transfer through the thickness of the specimen
  - Steady state conditions

$$q_{calc} = -\lambda_e(T)\frac{dT}{dx} \Rightarrow q_{calc} = -\frac{1}{L}\int_{T_0}^{T_L} \lambda_e(T)\,dT$$

L: Specimen's thickness

T_0: Temperature at position x=0 (exposed side)

T_L: Temperature at position x=L (ambient side)

λ_e: equivalent thermal conductivity

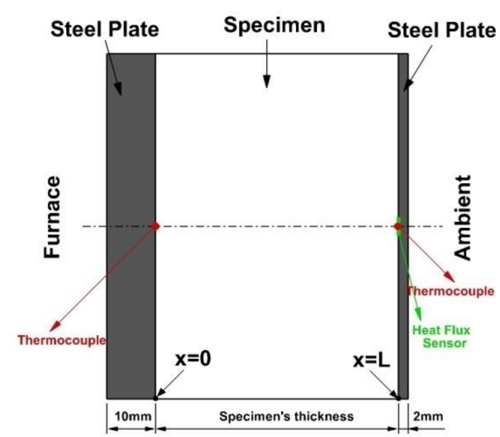

National Technical University of Athens

Main Idea

- Definition of thermal conductivity
  - Minimize the difference between the experimental and the calculated values of the steady state heat flux for all the experimental data set

$$e_q = \min_{\mathbf{x}} \sum_{i=1}^{N_{\exp}} \left(q_{\exp i} - q_{calc,i}(\mathbf{x})\right)^2$$

Related to the equivalent thermal conductivity

e_q: Error to be minimized

N_{exp}: Number of furnace's temperature levels (=9)

***X**: Vector of optimization parameters (independent variables)*

q_{exp}: Experimental heat flux

q_{calc}: Calculated heat flux

Equivalent thermal conductivity

$$\lambda_e = \lambda_s + \lambda_g + \lambda_c + \lambda_r$$

λ_e: Equivalent thermal conductivity

λ_s: Solid conduction (assumed to be constant)

λ_g: Gas conduction

λ_c: Gas convection (negligible for pore sizes smaller than 1μm)

λ_r: Radiation

Gas conduction

$$\lambda_g = \frac{\lambda_{g,0}(T)}{1 + \frac{2\beta k_B}{\sqrt{2}\pi d_g^2}\frac{T}{\delta P_g}}$$

$\lambda_{g,0}$: Air's thermal conductivity (W/mK)

β: Constant characterizing the efficiency of energy transfer when gas molecules hit the solid structure of the material (1.5≤β≤2.0)

k_B: Boltzman constant (1.38066 ×10^{-23}J/K)

d_g: Diameter of the gas molecules (3.53 ×10^{-10}m)

T: Temperature (K)

δ: Characteristic pore size (m)

P_g: Pressure (Pa)

At the examined temperature the VIP was considered to be at atmospheric pressure

Radiation

$$\lambda_g = \frac{16}{3}\frac{n^2 \sigma T^3}{E}$$

n: Index of refraction

σ: Stefan-Boltzman constant ($5.67 \times 10^{-8} W/m^2K^4$)

E: Extinction coefficient (m^{-1})

Equivalent thermal conductivity

$$\lambda_e = \lambda_s + \frac{\lambda_{g,0}(T)}{1 + \frac{2\beta k_B}{\sqrt{2}\pi d_g^2}\frac{T}{\delta P_g}} + \frac{16}{3}\frac{n^2 \sigma T^3}{E}$$

Equivalent thermal conductivity

$$\lambda_e = \lambda_s + \frac{\lambda_{g,0}(T)}{1+\dfrac{2\beta k_B}{\sqrt{2}\pi d_g^2}\dfrac{T}{\delta P_g}} + \frac{16}{3}\frac{n^2\sigma T^3}{E}$$

Optimization Parameters

$$e_q = \min_{\mathbf{x}} \sum_{i=1}^{N_{\exp}} \left(q_{\exp i} - q_{calc,i}(\mathbf{x})\right)^2$$

Equivalent thermal conductivity

$$\lambda_e = \lambda_s + \frac{\lambda_{g,0}(T)}{1 + \frac{2\beta k_B}{\sqrt{2}\pi d_g^2}\frac{T}{\delta P_g}} + \frac{16}{3}\frac{n^2\sigma T^3}{E}$$

Optimization Parameters

<u>*Ranges*</u>

1mW/mK≤ $\boldsymbol{\lambda_s}$*≤4mW/mK*

1≤ $\boldsymbol{\beta}$*≤3*

4000m^{-1}*≤* ***E****≤13000m*$^{-1}$

$$e_q = \min_{\mathbf{x}} \sum_{i=1}^{N_{\exp}} \left(q_{\exp i} - q_{calc,i}(\mathbf{x})\right)^2$$

- Introduction
- Experimental Methodology
- Numerical Modeling
- Results & Discussion
- Conclusions & Outlook

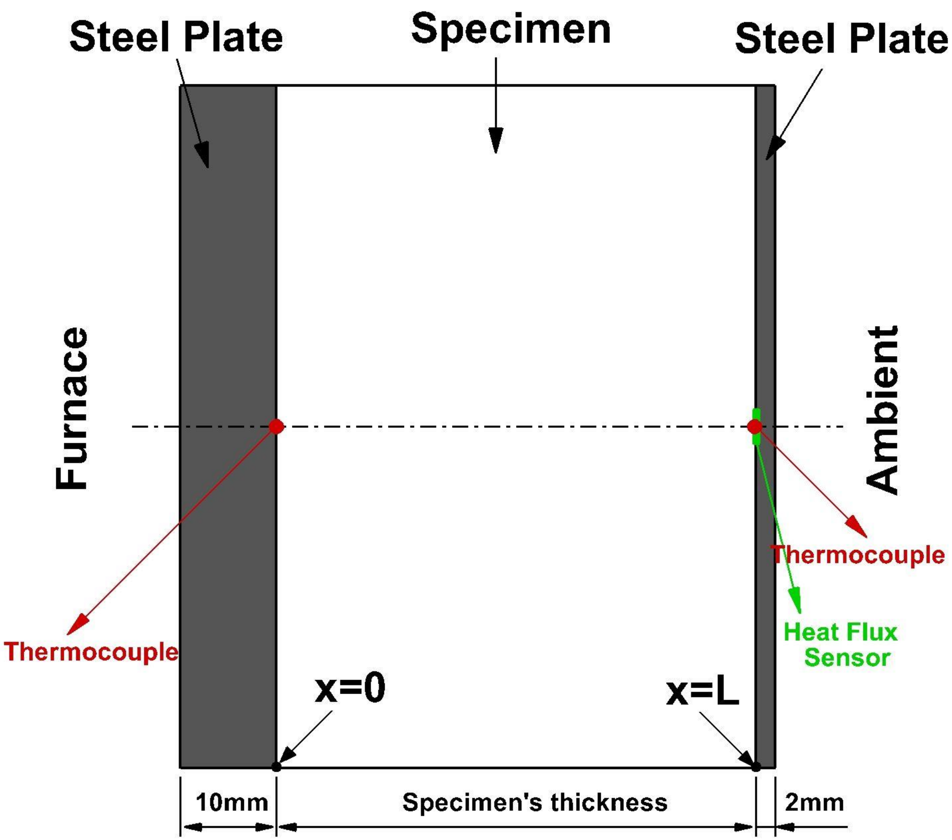

Schematic diagram of the experimental set up

$T_{furnace}$ (°C)	T_0 (°C)	T_L (°C)	q_L (W/m²)
100	101.9	24.2	40.9
200	197.9	29.7	86.6
300	294.9	35.5	129.2
400	391.0	40.7	176.3
500	488.8	47.0	231.6
600	587.2	53.6	299.3
700	682.5	61.4	381.6
800	771.2	70.1	490.4
900	860.5	81.4	633.1

Measured steady state temperatures and heat flux values for each temperature level of the furnace

- Experimental values used in the optimization process
  - MATLAB curve fitting tool
  - Optimization Parameters: **β=2, λ_s=2.1mW/mK, E=9305m^{-1}**
- Calculated heat flux values are in sound agreement with the respective experimental
- Small discrepancies are related to the assumption that the optimization parameters are temperature independent

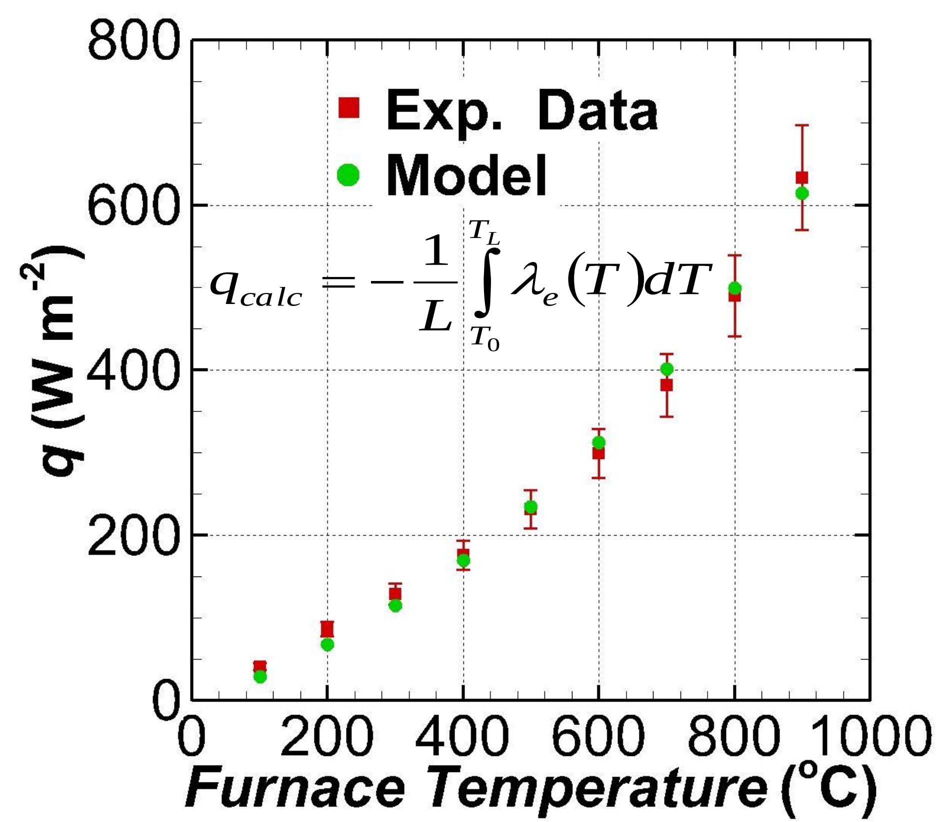

Comparison between the predicted and the experimental steady state heat flux values for all the temperature levels of the furnace

- Determination of the VIP's equivalent thermal conductivity
  - Temperatures up to 200°C – 250°C → main heat transfer mechanism is gas conduction
  - At temperatures between 250°C and 500°C → radiation mechanism increases its contribution
  - Temperatures above 500°C → radiation prevails against other heat transfer mechanisms

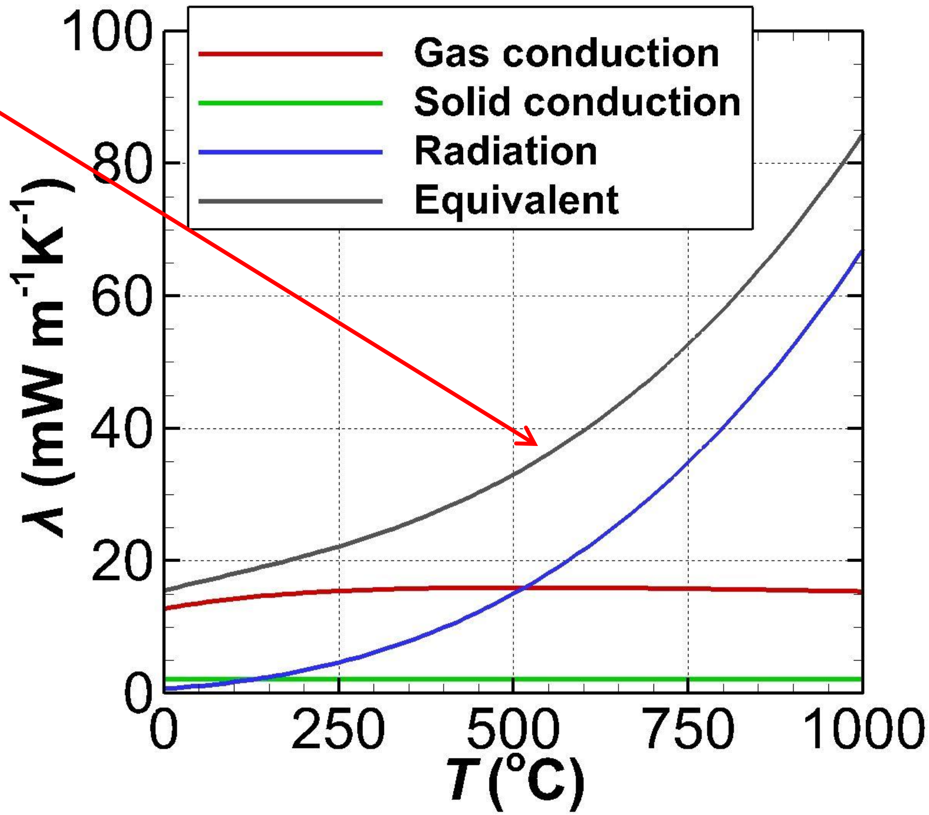

Contribution of each heat transfer mechanism to the equivalent thermal conductivity

- Determination of the VIP's equivalent thermal conductivity
  - Temperatures up to 200°C – 250°C → main heat transfer mechanism is gas conduction
  - At temperatures between 250°C and 500°C → radiation mechanism increases its contribution
  - Temperatures above 500°C → radiation prevails against other heat transfer mechanisms

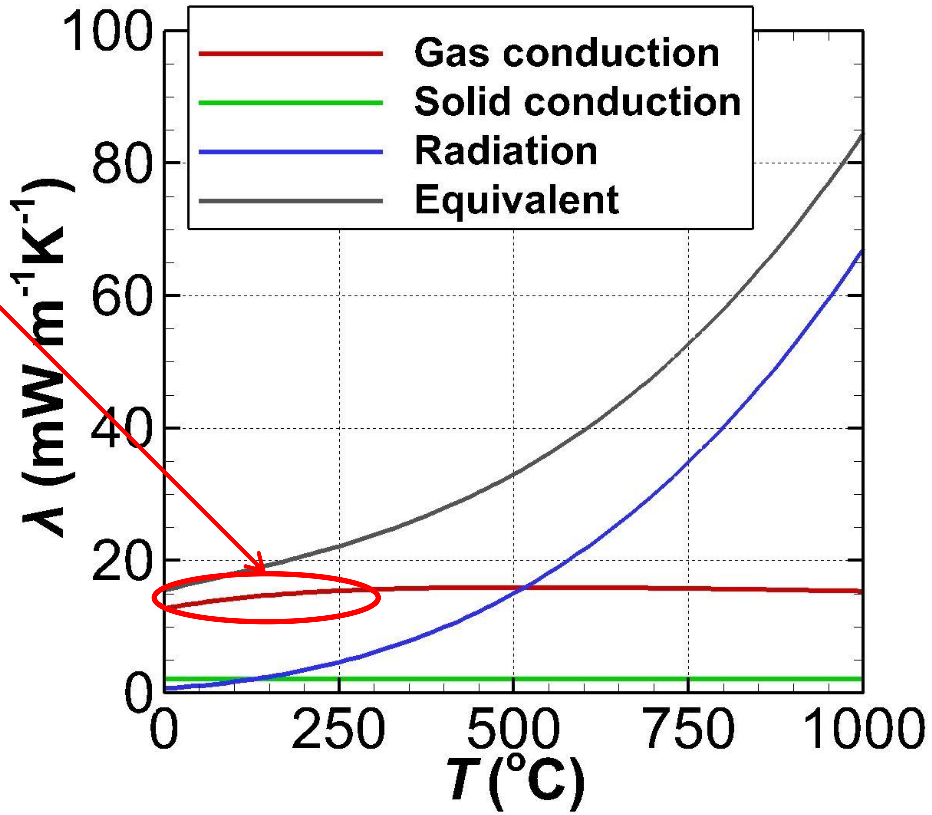

Contribution of each heat transfer mechanism to the equivalent thermal conductivity

- Determination of the VIP’s equivalent thermal conductivity
  - Temperatures up to 200°C – 250°C → main heat transfer mechanism is gas conduction
  - At temperatures between 250°C and 500°C → radiation mechanism increases its contribution
  - Temperatures above 500°C → radiation prevails against other heat transfer mechanisms

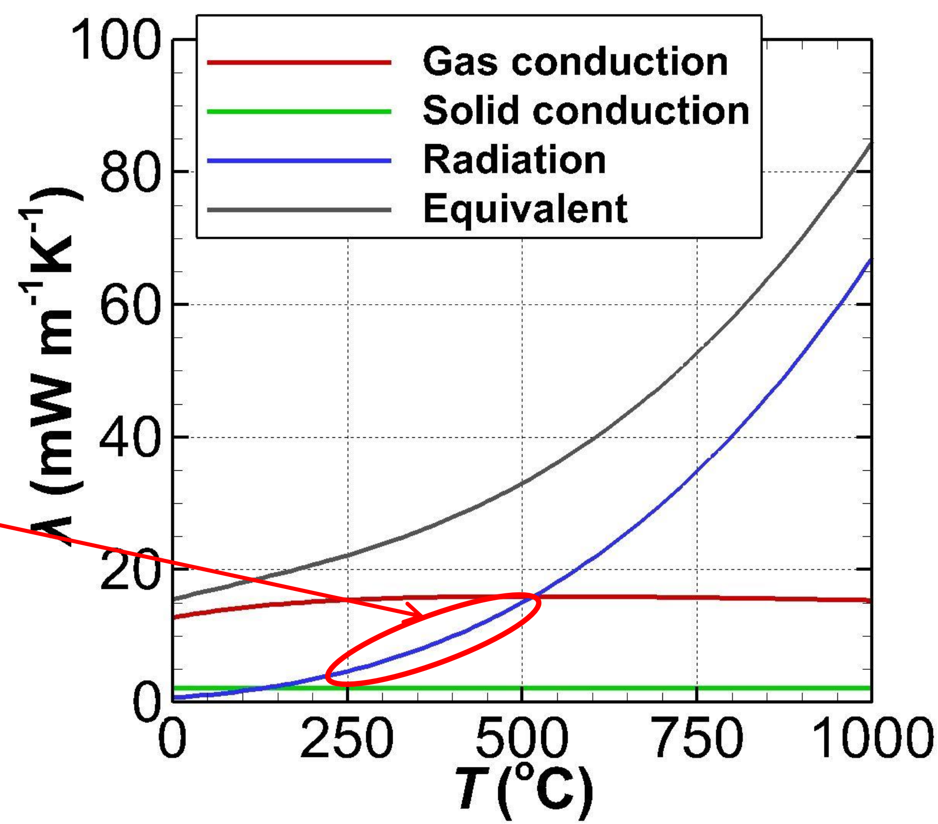

Contribution of each heat transfer mechanism to the equivalent thermal conductivity

- Determination of the VIP's equivalent thermal conductivity
  - Temperatures up to 200ºC – 250ºC → main heat transfer mechanism is gas conduction
  - At temperatures between 250ºC and 500ºC → radiation mechanism increases its contribution
  - Temperatures above 500ºC → radiation prevails against other heat transfer mechanisms

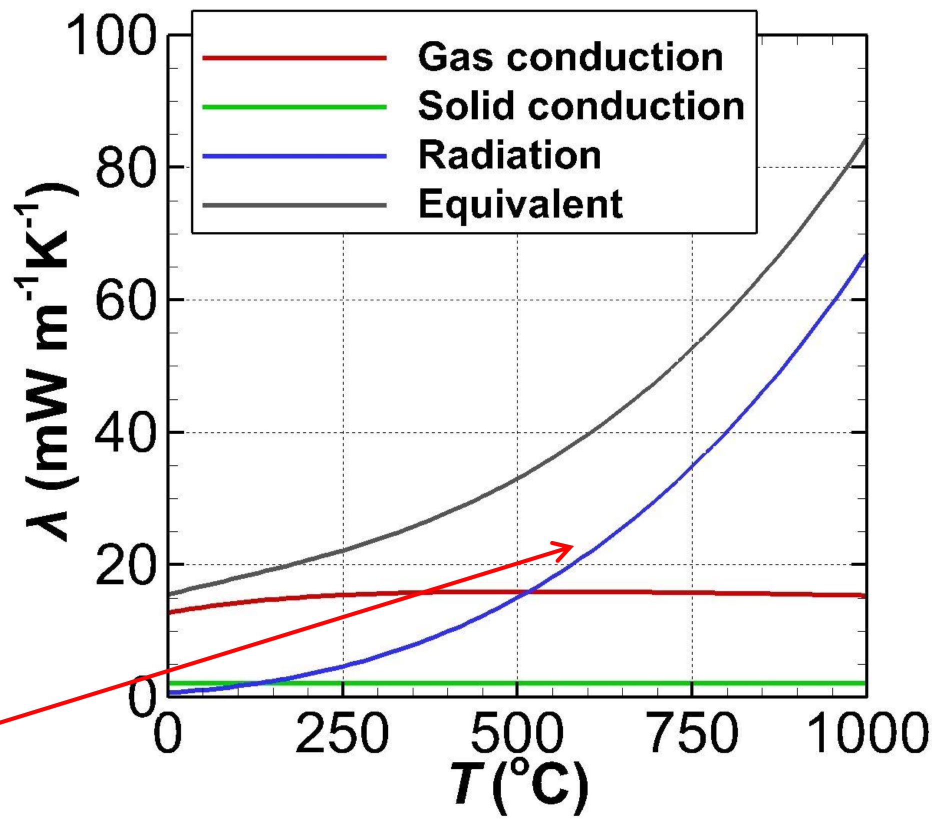

Contribution of each heat transfer mechanism to the equivalent thermal conductivity

- Further establishment of the findings
  - Comparison of the evacuated thermal conductivity, λ_{evac}, with respective experimental values from ANNEX 39
  - Defined λ_{evac} lies between the experimental data at temperatures up to 200°C

$$\lambda_{evac} = \lambda_s + \lambda_r$$

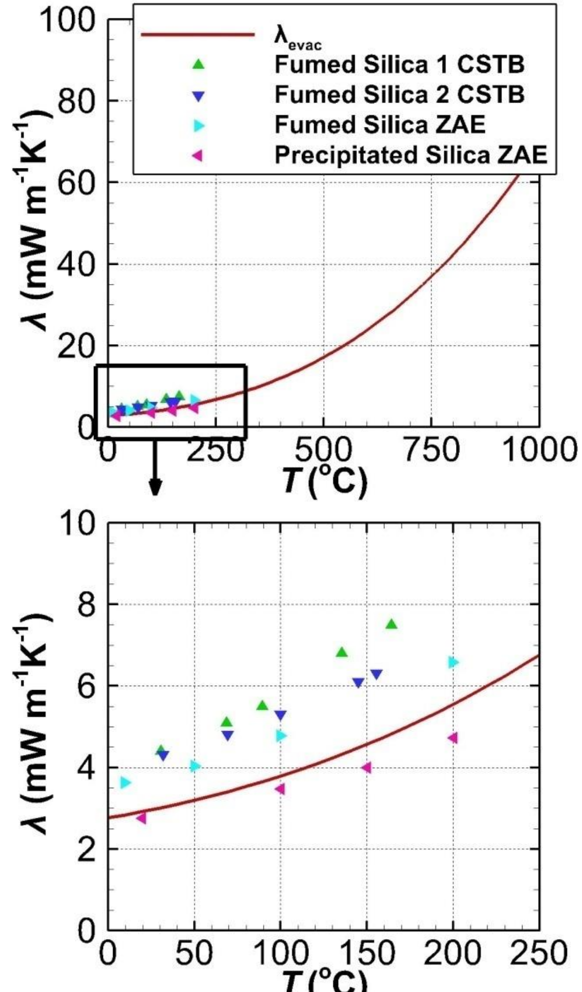

Comparison of the evacuated thermal conductivity with experimental data from ANNEX 39

- Introduction
- Experimental Methodology
- Numerical Modeling
- Results & Discussion
- **Conclusions & Outlook**

National Technical University of Athens

- Summary
  - Combined method (experimental and numerical) for the determination of the thermal conductivity of VIP at fire temperatures
  - Experimental method
    - Measurement of temperature and heat flux on the surfaces of VIP at several temperature levels
  - Numerical method
    - Comparison of the experimental data with detailed model
    - Optimization algorithm for the definition of the optimum parameters
- Conclusions
  - Proposed method **successfully employed** for the determination of the VIP's thermal conductivity at **temperatures up to 900°C**
  - Optimum model parameters: **β=2, λ_s=2.1mW/(mK), E=9305m^{-1}** (within the range given in ANNEX 65)
  - The thermal conductivity of VIP varies between **18mW/(mK) and 85mW/(mK)** for the temperature range 100°C – 900°C

QUESTIONS

Thank you for your attention

SHARE YOUR THOUGHTS

Acknowledgements

The authors acknowledge the financial support of the European Commission in the frame of the FP7-2013-NMP-ENV-EeB project 'ELISSA' (www.elissaproject.eu)